Centimeter-scale-diameter Co-based bulk metallic glasses with fracture strength exceeding 5000 MPa

ZHANG Tao[*], YANG Qin, JI YunFei, LI Ran, PANG ShuJie, WANG JianFeng & XU Tao

Key Laboratory of Aerospace Materials and Performance of Ministry of Education, School of Materials Science and Engineering, Beihang University, Beijing 100191, China

$Co_{48-x}Fe_xCr_{15}Mo_{14}C_{15}B_6Er_2$ ($x = 2.5$ and 5) bulk metallic glasses (BMGs) with critical size (d_c) up to 15 mm in diameter were synthesized by copper mold casting. $Co_{43}Fe_5Cr_{15}Mo_{14}C_{15}B_6Er_2$ BMG has a wide supercooled liquid region (84 K) and ultrahigh fracture strength exceeding 5000 MPa, which is the highest value for reported metallic glasses with d_c exceeding 1 cm. Furthermore, the Poisson ratio, Young modulus, shear modulus and bulk modulus of this alloy were evaluated to be 0.31, 217 GPa, 82 GPa and 214 GPa, respectively. The ideal configurational entropy of $Co_{48-x}Fe_xCr_{15}Mo_{14}C_{15}B_6Er_2$ ($x = 0$ and 5) has been calculated. The introduction of the similar element Fe in the Fe-free Co-Cr-Mo-C-B-Er alloy will be beneficial to increasing the ideal configurational entropy and depressing the critical cooling rate to achieve greater glass-forming ability. The combination of superior glass-forming ability and ultrahigh fracture strength makes the present $Co_{48-x}Fe_xCr_{15}Mo_{14}C_{15}B_6Er_2$ ($x = 2.5$ and 5) BMGs promising candidates as advanced structural materials.

bulk metallic glass, glass forming ability, mechanical properties, Co alloys

The mechanical properties of metallic glasses have been widely studied in recent years. It has been reported that fracture strength is in the range of 1500–2000 MPa for Zr-based metallic glasses [1–4], 1800–2400 MPa for Ti-based metallic glasses [5,6], 2000–2500 MPa for Cu-based metallic glasses [7,8], 3000–4000 MPa for Fe-based metallic glasses [9–11], and 4000–6000 MPa for Co-based metallic glasses [12–14]. In contrast with conventional crystalline alloys, monolithic metallic glasses have exceptionally high fracture strengths. It is therefore expected that those metallic glasses can be used as structural materials.

Currently, one obstacle that restricts the industrial application of metallic glasses as structural materials is their limited glass-forming ability (GFA). It is believed that there is a large atomic size difference and negative heats of mixing among the main constituent elements, which can be defined as dissimilar elements, in good glass-forming alloys [15].

During the last decade, bulk metallic glasses (BMGs) with critical diameter mainly of the millimeter scale and occasionally of the centimeter scale, which satisfy this compositional criterion have been discovered [2,4,5,7,9]. Recently, we found that the GFA of some glassy alloys consisting of dissimilar elements can be improved when elements with atomic sizes and chemical properties similar to those of the components are added [16–20]. Using this new concept of the coexistence of similar and dissimilar elements, we have synthesized many BMGs with superior GFA; e.g. the critical diameter of La-Ce-Al-Co-Cu BMGs reaches 32 mm [18].

The aim of this research is to develop BMGs with high fracture strength exceeding 5000 MPa and high GFA with critical diameter exceeding 1 cm. Despite there being an increasing number of research papers on the mechanical properties of BMGs, only Co-based BMGs have been reported to exhibit ultrahigh strengths up to 5–6 GPa in a compression test [12,14]. Recently, our group reported that

$Co_{48}Cr_{15}Mo_{14}C_{15}B_6Er_2$ BMGs with superior GFA can be produced in bulk form with critical thickness of 10 mm [21,22]. Therefore, $Co_{48}Cr_{15}Mo_{14}C_{15}B_6Er_2$ alloy was chosen as the starting composition and Fe was introduced as a similar element to partially substitute Co. The GFA of $Co_{48-x}Fe_x$-$Cr_{15}Mo_{14}C_{15}B_6Er_2$ ($x = 2.5$ and 5) alloys can be improved by the substitution of Fe for Co. Moreover, the present BMGs exhibit ultrahigh fracture strength exceeding 5000 MPa.

1 Experimental

$Co_{48-x}Fe_xCr_{15}Mo_{14}C_{15}B_6Er_2$ ($x = 2.5$ and 5) alloy ingots were prepared by arc-melting the mixtures of pure Co, Fe, Cr, Mo, C, B and Er (all with purity of 99.9 mass %) metals in a high-purity argon atmosphere. The ingots were remelted at least four times to ensure their chemical homogeneity. From the master alloys, cylindrical rods were fabricated by copper mold casting under a high-purity argon atmosphere. Cross sections of the as-cast rods were examined by X-ray diffraction (XRD) using a Rigaku D/max 2200 PC automatic X-ray diffractometer with Cu Kα radiation to study the structure. $Co_{43}Fe_5Cr_{15}Mo_{14}C_{15}B_6Er_2$ glassy alloy with diameter of 15 mm was observed with a JEM-2100F transmission electron microscope at an operating voltage of 200 kV. The thermal stability was examined by NETZSCH DSC 404C differential scanning calorimetry (DSC) at a heating rate of 0.33 K/s. Fracture strength was measured by an Instron testing machine. The specimens were 1 mm in diameter and 2 mm in length, and the strain rate was 4.2×10^{-4} s^{-1}. Nanoindentation experiments were conducted at room temperature using an ENT-1100a nanoindenter. The density (ρ) was measured employing the Archimedes technique using a Mettler Toledo balance (readability: 0.1 μg). Elastic constants (Poisson's ratio v, Young's modulus E, shear modulus G and bulk modulus B) were determined from the density and velocities of the longitudinal wave (V_L) and transverse wave (V_T) in the material with an Olympus Panametrics-NDT 5900 PR ultrasonic testing device. The latter were measured employing a pulse-echo ultrasonic echography technique in infinite mode and in reflection mode via coupling gels. v, E, G and B can be calculated from [23]:

$$v = \frac{1 - 2r^2}{2 - 2r^2}, \tag{1}$$

$$E = V_T^2 \rho \frac{(1+v)(1-2v)}{1-v}, \tag{2}$$

$$G = \frac{E}{2(1+v)}, \tag{3}$$

$$B = \frac{E}{3(1-2v)}, \tag{4}$$

where $r = V_T/V_L$. The error bands of the calculation elastic constants are below 5%.

2 Results and discussion

XRD patterns of as-cast $Co_{48-x}Fe_xCr_{15}Mo_{14}C_{15}B_6Er_2$ ($x = 2.5$ and 5) cylindrical samples with different diameters are shown in Figure 1. No appreciable peaks are detected for the samples of $Co_{45.5}Fe_{2.5}Cr_{15}Mo_{14}C_{15}B_6Er_2$ with diameter of 12 mm and $Co_{43}Fe_5Cr_{15}Mo_{14}C_{15}B_6Er_2$ with diameter of 15 mm within the resolution limit of the XRD, which indicates fully amorphous structure.

It has been pointed out that alloys with microcrystalline phase can also exhibit broad diffraction halos like those of metallic glass. During DSC scanning, however, metallic glasses exhibit exothermic peaks, while microcrystalline materials have monotonically decaying heat flow signals [7]. Hence, DSC scanning was performed in the present study. The DSC curves of a $Co_{43}Fe_5Cr_{15}Mo_{14}C_{15}B_6Er_2$ ribbon sample and cylindrical sample with diameter of 15 mm are shown in Figure 2. Apparent exothermic peak characteristics of crystallization processes confirm the glassy structure of the samples. No obvious difference is detected between DSC traces of the ribbon and cylindrical samples, indicating similar glass states. In addition, the Co-based BMG has high-thermal-stability characteristics of a high glass transition temperature (T_g) of 844 K and wide supercooled liquid region (ΔT_x, $\Delta T_x = T_g - T_x$, where T_x is the onset temperature of crystallization) of 84 K, and it is thus useful in thermoplastic applications as a nano-molding material [24,25].

To further clarify the microstructure, a high-resolution transmission electron microscope (HRTEM) image with a selected-area electron diffraction (SAED) pattern (inset) of the as-cast $Co_{43}Fe_5Cr_{15}Mo_{14}C_{15}B_6Er_2$ sample with diameter
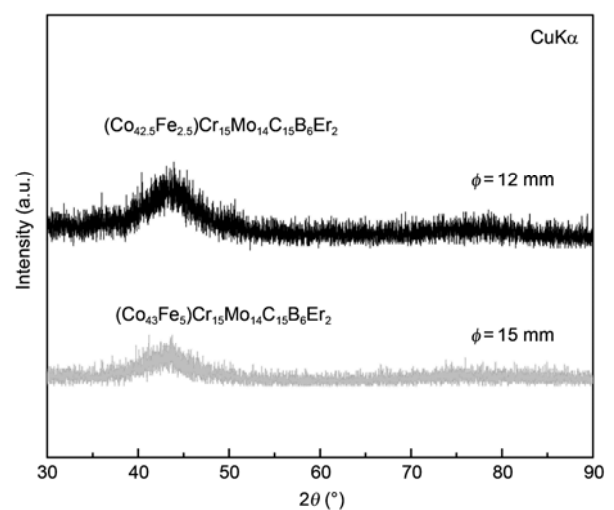
Figure 1 X-ray diffraction (XRD) patterns of as-cast $Co_{48-x}Fe_xCr_{15}Mo_{14}$-$C_{15}B_6Er_2$ ($x = 2.5$ and 5) cylindrical samples in different diameters.
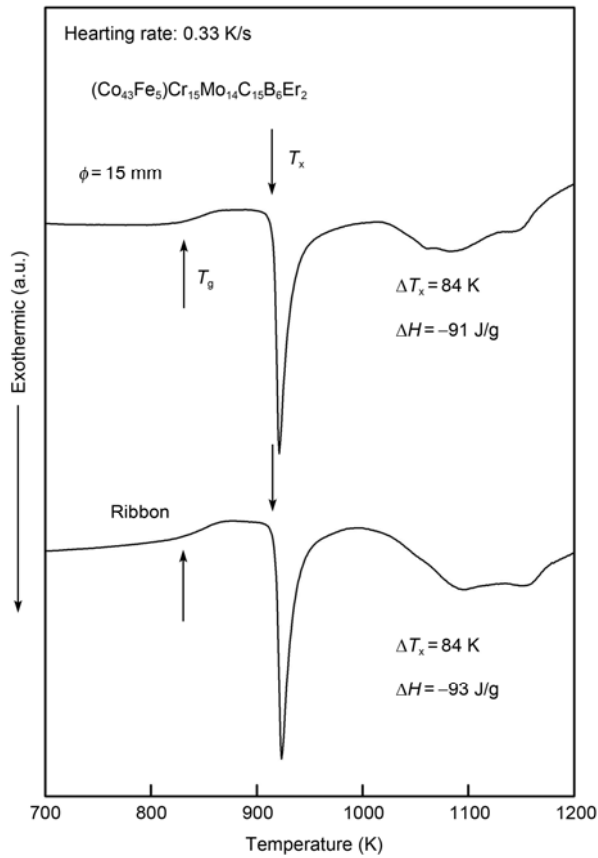
Figure 2   DSC traces for $Co_{43}Fe_5Cr_{15}Mo_{14}C_{15}B_6Er_2$ ribbon and cylindrical sample with diameter of 15 mm.

Figure 3   High-resolution transmission electron microscope (HRTEM) image and selected area electron diffraction (SAED) pattern (inset) of the as-cast sample of $Co_{43}Fe_5Cr_{15}Mo_{14}C_{15}B_6Er_2$ alloy in diameter of 15 mm.

of 15 mm is shown in Figure 3. The SAED pattern exhibits only a halo ring, which is inherent to a glassy phase, and indicates no distinguishable crystals presenting in the sample. The HRTEM image c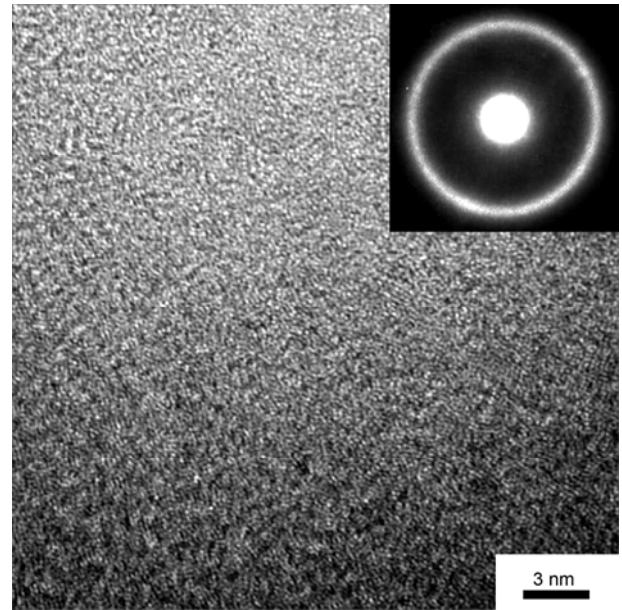onfirms that there are no distin-guishable crystals on the nanometer scale. Integrating the results of XRD, DSC and transmission electron microscopy, it is concluded that the critical diameter of $Co_{43}Fe_5Cr_{15}Mo_{14}$-$C_{15}B_6Er_2$ BMG can reach 15 mm.

Figure 4 shows the mixing enthalpy of constituents in the (Co, Fe)-Cr-Mo-C-B-Er alloys. It is found that the mixing enthalpies are -24 kJ/mol for the Co–Er pair, -19 kJ/mol for the B–Mo pair, -16 kJ/mol for the Cr–B pair, -11 kJ/mol for the B–Fe pair and -9 kJ/mol for the Co–B pair. The large negative mixing enthalpies for constituent elements of
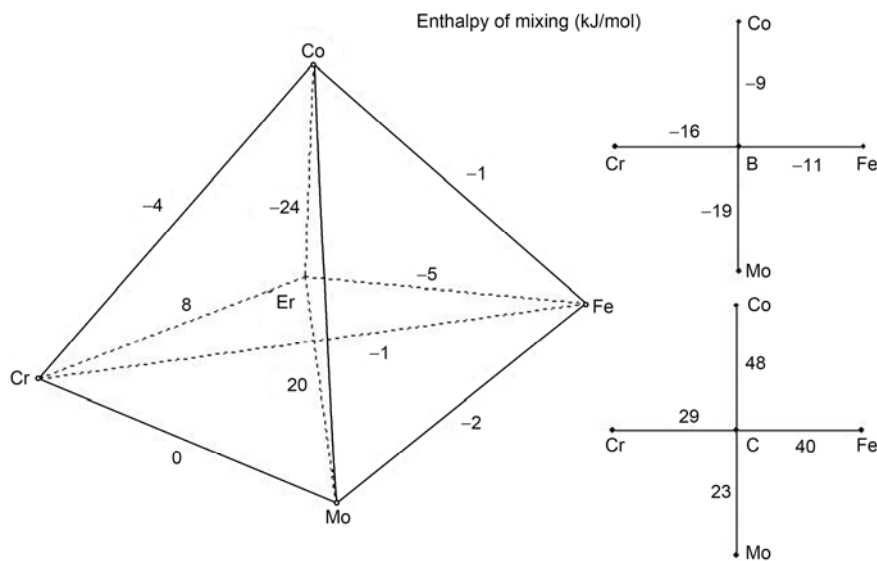

Figure 4   Mixing enthalpy of the constituents in (Co, Fe)-Cr-Mo-C-B-Er alloys.

the present BMGs indicate strong cohesive forces, and lead to dense packing in the liquid state, which is favorable for glass formation during solidification [15].

The reason that the Fe-containing alloy has greater GFA than the Fe-free alloy ($Co_{48}Cr_{15}Mo_{14}C_{15}B_6Er_2$) is discussed on the basis of thermodynamics. It has been reported that the maximum thickness of a metallic glass (D_c) can be determined as [26]:

$$R_c (K/s) = 10/D_c^2 (cm), \qquad (5)$$

where R_c is the critical cooling rate. In accordance with classical crystallization theory, R_c for metallic glasses can be written as [27–29]:

$$R_c = Z \frac{k_B T_m^2}{a^3 \eta_{T=T_m}} \exp\left[f_1\left(\frac{\Delta H - T_m \Delta S^{ideal}}{300R}\right) - f_2\left(\frac{T_m S_\sigma}{300R}\right)\right], \quad (6)$$

where Z is a constant, taken as 2×10^{-6}, k_B is Boltzmann's constant, a is the average interatomic distance, η is the viscosity, ΔH is the mixing enthalpy of the system, ΔS^{ideal} is the ideal configurational entropy, S_σ is the mismatch term of entropy and R is the gas constant. Employing the method of least squares, f_1 and f_2 were calculated to be 0.75 and 1.2, respectively [27–29].

According to the regular solution model, ΔH and ΔS^{ideal} are defined for multi-component systems with N elements [27–29]:

$$\Delta H = \sum_{i=1,i\neq j}^N \Omega_{ij} c_i c_j, \qquad (7)$$

$$\Delta S^{ideal} = -R\sum_{i=1}^N (c_i \ln c_i), \qquad (8)$$

where R is the gas constant, c_i is the mole fraction of i, and Ω_{ij} is the regular solution interaction parameter between elements i and j. Ω_{ij} can be calculated as

$$\Omega_{ij} = 4\Delta H_{AB}^{mix}. \qquad (9)$$

The relation follows from the definition in eq. (7) for the equal-atomic composition of a binary A-B system, and ΔH_{AB}^{mix} is the mixing enthalpy of the binary A-B system. In our previous research, T_m and ΔS^{ideal} were confirmed to be the primary factors resulting in the difference in R_c among alloys with similar elements coexisting. According to eq. (6), alloys with higher ΔS^{ideal} always exhibit lower R_c and greater GFA. In the present study, the ideal configuration entropy of Fe-containing alloy calculated from eq. (8) is 13.34 J/(mol K), higher than that of Fe-free alloy (12.01 J/(mol K)). T_m of Fe-containing alloy is 1365 K, higher than that of Fe-free alloy (1350 K). Assuming the two alloys possess similar values for other factors, such as the average interatomic distance and viscosity, the ratio of R_c (Fe-containing alloy) to R_c (Fe-free alloy) can be calculated as

$$\frac{R_c (\text{Fe-containing alloy})}{R_c (\text{Fe-free alloy})} \approx \frac{1365^2}{1350^2}$$

$$\exp\left[0.75\times\frac{1350\times12.01-1365\times13.34}{300\times8.314}\right] = 0.56. \qquad (10)$$

According to eq. (5), the ratio of D_c (Fe-containing alloy) to D_c (Fe-free alloy) can be calculated as

$$\frac{D_c (\text{Fe-containing alloy})}{D_c (\text{Fe-free alloy})} = \sqrt{\frac{R_c (\text{Fe-free alloy})}{R_c (\text{Fe-containing alloy})}} = 1.34. \qquad (11)$$

This value is in good agreement with the experimental results (15/10=1.5) in the present work. Thus, the decrease in the critical cooling rate resulting from the configurational entropy can reasonably explain the obvious improvement in GFA of the Co-based alloy for this substitution.

Figure 5 shows compressive stress-strain curves for the $Co_{48-x}Fe_xCr_{15}Mo_{14}C_{15}B_6Er_2$ ($x = 2.5$ and 5) bulk metallic glasses with diameter of 1 mm. Both samples present elastic deformation with an increase in compressive stress, followed by final abrupt fracture, and as a result, the rods break into pieces. For reported BMGs with critical diameter exceeding 1 cm, such as $Mg_{54}Cu_{26.5}Ag_{8.5}Gd_{11}$, $Pd_{40}Cu_{30}Ni_{10}P_{20}$, $Zr_{65}Al_{7.5}Ni_{10}Cu_{17.5}$ and $Fe_{41}Co_7Cr_{15}Mo_{14}B_6Y_2$, the fracture strengths range from 1000 to 3400 MPa [2,10,30,31]. In the present study, the fracture strength of $Co_{43}Fe_5Cr_{15}Mo_{14}C_{15}B_6Er_2$ BMG is 5200 MPa, which is the highest among amorphous alloys with critical diameter exceeding 1 cm so far.

To further investigate the fracture behavior of the $Co_{43}Fe_5Cr_{15}Mo_{14}C_{15}B_6Er_2$ BMG, nanoindentation experiments were carried out on 4 mm rods in a load-control mode. A typical load-displacement (P-h) curve obtained in a nanoindentation test is shown in Figure 6. There are several discontinuities in the curve (marked by arrows), the presence of which are known as the "pop-in" effect. During this
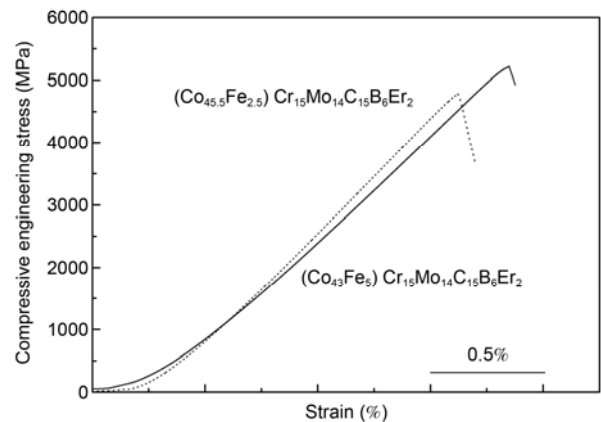

Figure 5   Compressive stress-strain curves of $Co_{48-x}Fe_xCr_{15}Mo_{14}C_{15}B_6Er_2$ ($x=2.5$ and 5) metallic glasses with diameter of 1 mm.
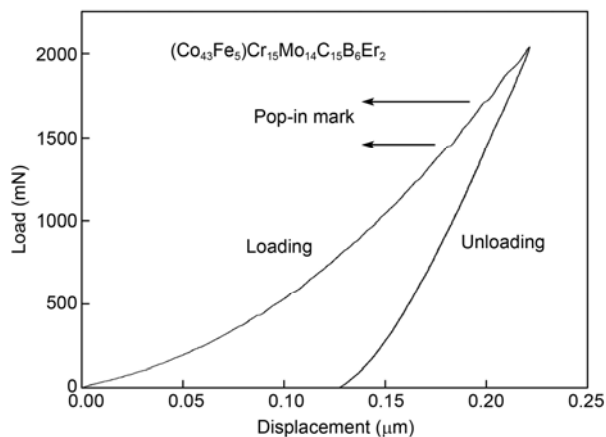
Figure 6 Load-displacement (*P-h*) curve of $Co_{43}Fe_5Cr_{15}Mo_{14}C_{15}B_6Er_2$ metallic glass with diameter of 4 mm.

period, the displacement of the indenter increases with little or no change in the load, indicating microplastic deformation.

Ultrasonic measurements were carried out to determine the elastic constants of $Co_{43}Fe_5Cr_{15}Mo_{14}C_{15}B_6Er_2$ BMG with density $\rho = 8.36$ g cm^{-3}. The Poisson ratio, Young modulus, shear modulus and bulk modulus were calculated to be 0.331, 217 GPa, 82 GPa and 214 GPa, respectively. Figure 7 shows good correlation between the fracture strength and Young's modulus for typical metallic glasses and the present BMGs. The Co-based BMGs have high fracture strength and Young's modulus among the present metallic glasses. It has been pointed out by Inoue et al. that electrons of the metalloid elements can transfer from the original element to the *d* shells of transition metal elements to form *s-d* hybrid bonds [13]. In the present study, there is strong interaction between metalloid atoms (B) and the metal (Co and Fe) through *s-d* hybrid bonding, which results in the high strength of the $Co_{48-x}Fe_xCr_{15}Mo_{14}C_{15}B_6Er_2$ ($x = 2.5$ and 5) BMG.
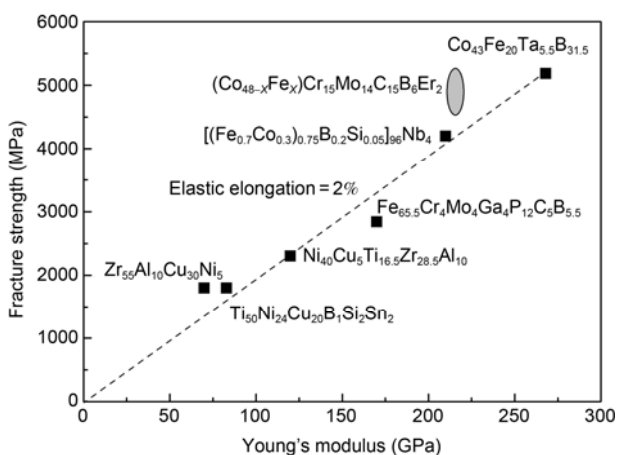

Figure 7 Correlation between fracture strength and Young's modulus for typical metallic glasses.

3 Conclusions

$Co_{48-x}Fe_xCr_{15}Mo_{14}C_{15}B_6Er_2$ ($x = 2.5$ and 5) BMGs with ultrahigh strength exceeding 5000 MPa and high thermal stability can be formed with diameters exceeding 1 cm by copper mold casting. The Poisson ratio, Young modulus, shear modulus and bulk modulus of the alloy with $x = 5$ were determined to be 0.331, 217 GPa, 82 GPa and 214 GPa, respectively. The high GFA and ultrahigh strength of the $Co_{48-x}Fe_xCr_{15}Mo_{14}C_{15}B_6Er_2$ ($x = 2.5$ and 5) BMGs can be attributed to the large negative mixing enthalpies among the constituent elements and strong chemical bonds between B and Co/Fe. These Co-based BMGs with combination of superior GFA and ultrahigh strength are promising for further applications as structural materials.

1 Inoue A, Zhang T, Masumoto T. Amorphous Zr-Al-TM (TM=Co, Ni, Cu) Alloys with significant supercooled liquid region of over 100 K. Mater Trans JIM, 1991, 32: 1005–1010

2 Inoue A, Zhang T, Nishiyama N, et al. Preparation of 16 mm diameter rod of amorphous $Zr_{65}A_{17.5}Ni_{10}Cu_{17.5}$ alloy. Mater Trans JIM, 1993, 34: 1234–1237

3 Li Y H, Zhang W, Dong C, et al. Unusual compressive plasticity of a centimeter-diameter Zr-based bulk metallic glass with high Zr content. J Alloy Comp, 2010, 540: S2–S5

4 Inoue A, Zhang T. Fabrication of bulk glassy $Zr_{55}Al_{10}Ni_5Cu_{30}$ alloy of 30 mm in diameter by a suction casting method. Mater Trans JIM, 1996, 37: 185–187

5 Guo F Q, Wang H J, Poon S J, et al. Ductile titanium-based glassy alloy ingots. Appl Phys Lett, 2005, 86: 091907

6 Wu X F, Suo Z Y, Si Y, et al. Bulk metallic glass formation in a ternary Ti-Cu-Ni alloy system. J Alloy Comp, 2008, 452: 268–272

7 Xu D H, Duan G, Johnson W L. Unusual glass-forming ability of bulk amorphous alloys based on ordinary metal copper. Phys Rev Lett, 2004, 92: 245505

8 Choi-Yim H, Conner R D. Amorphous alloys in the Cu-Hf-Ti. J Alloy Comp, 2008, 459: 160–162

9 Lu Z P, Liu C T, Thompson J R, et al. Structural amorphous steels. Phys Rev Lett, 2004, 92: 245503

10 Shen J, Chen Q J, Sun J F, et al. Exceptionally high glass-forming ability of an FeCoCrMoCBY alloy. Appl Phys Lett, 2005, 86: 151907

11 Li L, Liu Y, Zhang T H, et al. Deformation behavior of Fe-based bulk metallic glass during nanoindentation. Sci China Ser G-Phys Mech Astron, 2008, 51: 365–371

12 Inoue A, Shen B L, Koshiba H, et al. Ultra-high strength above 5000 MPa and soft magnetic properties of Co-Fe-Ta-B bulk glassy alloys. Acta Mater, 2004, 52: 1631–1637

13 Chang C T, Shen B L, Inoue A. Co-Fe-B-Si-Nb bulk glassy alloys with superhigh strength and extremely low magnetostriction. Appl Phys Lett, 2006, 88: 011901

14 Wang J F, Li R, Hua N B, et al. Co-based ternary bulk metallic glasses with ultrahigh strength and plasticity. J Mater Res, 2011, 26: 2072–2079

15 Inoue A, Takeuchi A. Compositions, structure and glass-forming ability of bulk glassy alloys. Metastable and Nanostructured Materials-Nanomat-2001, Proceedings, 2002, 403: 1–11

16 Li R, Liu F J, Pang S, et al. The influence of similar element coexist-

ence in (La-Ce)-Al-(Co-Cu) bulk metallic glasses. Mater Trans, 2007, 48: 1680–1683

17 Li R, Pang S J, Ma C L, et al. Influence of similar atom substitution on glass formation in (La-Ce)-Al-Co bulk metallic glasses. Acta Mater, 2007, 55: 3719–3726

18 Zhang T, Li R, Pang S J. Effect of similar elements on improving glass-forming ability of La-Ce-based alloys. J Alloy Comp, 2009, 483: 60–63

19 Ji Y F, Pang S J, Zhang T. Enhanced glass-forming ability of a Sm-based alloy with the addition of La. J Alloy Comp, 2010, 505: 497–500

20 Li R, Yang Q, Pang S J, et al. Misch metal based metallic glasses. J Alloy Comp, 2008, 450: 181–184

21 Men H, Pang S J, Li R, et al. Crystallization kinetics of $Co_{48}Cr_{15}Mo_{14}C_{15}B_6Er_2$ bulk metallic glass with high thermal stability. Chin Phys Lett, 2006, 23: 417–419

22 Men H, Pang S J, Zhang T. Effect of Er doping on glass-forming ability of $Co_{50}Cr_{15}Mo_{14}C_{15}B_6$ alloy. J Mater Res, 2006, 21: 958–961

23 Li R, Stoica M, Wang G, et al. Glass formation, thermal properties, and elastic constants of La-Al-Co alloys. J Mater Res, 2010, 25: 1398–1404

24 Kumar G, Tang H X, Schroers J. Nanomoulding with amorphous metals. Nature, 2009, 457: 868–872

25 Kumar G, Schroers J. Write and erase mechanisms for bulk metallic glass. Appl Phys Lett, 2008, 92: 031901

26 Lin X H, Johnson W L. Formation of Ti-Zr-Cu-Ni bulk metallic glasses. J Appl Phys, 1995, 78: 6514–6519

27 Takeuchi A, Inoue A. Evaluation of glass-forming ability for metallic glasses from time-reduced temperature-transformation diagram. Mater Trans, 2001, 42: 2374–2381

28 Takeuchi A, Yubuta K, Makino A, et al. Evaluation of glass-forming ability of binary metallic glasses with liquidus temperature, crystallographic data from binary phase diagrams and molecular dynamics simulations. J Alloy Comp, 2009, 483: 102–106

29 Takeuchi A, Inoue A. Quantitative evaluation of critical cooling rate for metallic glasses. Mater Sci Eng A, 2001, 304: 446–451

30 Pan D G, Liu W Y, Zhang H F, et al. Mg-Cu-Ag-Gd-Ni bulk metallic glass with high mechanical strength. J Alloy Comp, 2007, 438: 142–144

31 Inoue A, Nishiyama N, Kimura H. Preparation and thermal stability of bulk amorphous $Pd_{40}Cu_{30}Ni_{10}P_{20}$ alloy cylinder of 72 mm in diameter. Mater Trans JIM, 1996, 37: 181–184